Continued meltwater influence on North Atlantic Deep Water instabilities during the early Holocene

ARTICLE *in* MARINE GEOLOGY · FEBRUARY 2015

Impact Factor: 2.2 · DOI: 10.1016/j.margeo.2014.11.015

3 AUTHORS, INCLUDING:

Aurora Elmore

Durham University

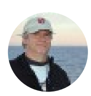

James D Wright

Rutgers, The State University of New Jersey

Marine Geology 360 (2015) 17–24

Contents lists available at ScienceDirect

Marine Geology

journal homepage: www.elsevier.com/locate/margeo

Continued meltwater influence on North Atlantic Deep Water instabilities during the early Holocene

A.C. Elmore [a,b,*], J.D. Wright [a], J. Southon [c]

[a] Department of Earth and Planetary Sciences, Rutgers University, New Brunswick, NJ, USA
[b] Department of Geography, Durham University, Durham, UK
[c] Earth System Science Department, University of California, Irvine, Irvine, CA, USA

ARTICLE INFO

Article history:
Received 2 March 2014
Received in revised form 26 November 2014
Accepted 30 November 2014
Available online 5 December 2014

Keywords:
Holocene
meltwater
North Atlantic

ABSTRACT

The transition into the Holocene marks the last large, orbitally derived climatic event and ultimately led to the onset of modern oceanic conditions. The influence of this climatic change on North Atlantic Deep Water (NADW) formation and circulation remains ambiguous. High-resolution records from southern Gardar Drift, south of Iceland, show abrupt decreases in benthic foraminiferal $\delta^{13}C$ values at discrete intervals during the early Holocene, suggesting that NADW shoaled episodically. Intervals of lower $\delta^{13}C$ values are coincident with higher $\Delta\delta^{18}O_{N.\ pachyderma\ (s)-G.\ bulloides}$ and high abundance of lithic grains/g, indicating that these periods also had enhanced surface water stratification, due to increased meltwater in the circum-North Atlantic region. Our new high-resolution planktonic and benthic foraminiferal stable isotopic data show that increased meltwater delivery led to brief reorganizations of deepwater currents. These southern Gardar surface and deep water records indicate that the early Holocene was a period of multiple abrupt climatic events that were propagated to the North Atlantic during the final break up of ice sheets in the Northern Hemisphere, and suggest that some component of the residual early Holocene sea level rise can be attributed to Northern Hemispheric sources.

1. Introduction

In the circum-North Atlantic region, the onset of the Holocene (~11.7 ka; Steffensen et al., 2008; Walker et al., 2009) marks the end of the transition from the last glacial period to current interglacial conditions (Broecker et al., 1989). Greenland ice core $\delta^{18}O$ records show that the Holocene was a warmer, less dusty period with decreased climatic variability, compared to the last glacial (Grootes et al., 1993; Alley et al., 1995). Similarly, geologic evidence from oceanic sediment cores (Broecker et al., 1989) and terrestrial records (Atkinson et al., 1987; Dansgaard et al., in press; Davis et al., 2003) from around the North Atlantic prescribe the Holocene as a period with warm temperatures and without large-scale climatic changes. The Holocene Thermal Maximum, caused by peak insolation ranged from 11 to 6 ka, depending on geographic location, and was less than 2 °C warmer than the Holocene baseline temperature in most locations (Kaufman et al., 2004; Renssen et al., 2012). Despite relative climatic stability, an estimated 30 m of lingering deglacial sea level rise occurred throughout the early Holocene, from 11.7 ka until at least ~8.0 ka (Fairbanks, 1989; Peltier and Fairbanks, 2006; Bard et al., 2010; Deschamps et al., 2012), attributed to freshwater delivery from the melting ice sheets (Andrews and Dunhill, 2004; Tornqvist and Hijma, 2012; Seidenkrantz et al., 2013). This evidence suggests that episodic or continual meltwater has been released from the Northern Hemisphere ice sheets, and may have affected North Atlantic ocean hydrography/circulation during the early Holocene.

Recent, higher-resolution examinations have demonstrated that Holocene climate is more variable than previously thought (e.g. Bond et al., 1997; Bianchi and McCave, 1999; Hoogakker et al., 2011; Larsen et al., 2012; Walker et al., 2012; Miller and Chapman, 2013), and have identified abrupt climate events within this purportedly stable interglacial period that have affected the deep ocean, as well as the more variable surface ocean (Alley et al., 1997; Marcott et al., 2013). Perhaps the most discussed of these is termed the '8.2 ka Event' (Alley et al., 1997; Rohling and Pälike, 2005; Cronin et al., 2007; Born and Levermann, 2010; Young et al., 2012; Liu et al., 2013), a climatic cooling caused by North Atlantic surface water freshening (Ellison et al., 2006) that has been attributed to meltwater release from glacial Lake Aggasiz (Barber et al., 1999; Hillaire-Marcel et al., 2007; Tornqvist and Hijma, 2012). This meltwater event delivered freshwater into the North Atlantic region, and may have disrupted thermohaline circulation (Renssen et al., 2001) and decreased NADW formation (Ellison et al., 2006; Kleiven et al., 2008), despite some evidence for faster Iceland–Scotland Overflow (Bianchi and McCave, 1999). This proposed mechanism for the 8.2 ka Event is similar to a proposed mechanism for Younger Dryas cooling, wherein Broecker et al. (1989) suggested that a 'fresh water

* Corresponding author at: Department of Geography, Durham University, Durham, UK. Tel.: +44 191 33 41931.
E-mail address: aurora.elmore@durham.ac.uk (A.C. Elmore).

http://dx.doi.org/10.1016/j.margeo.2014.11.015
0025-3227/

cap' in the northern North Atlantic would have altered deepwater formation for the duration of the Younger Dryas (Clark et al., 2001; McManus et al., 2004; Tarasov and Peltier, 2005; Elmore and Wright, 2011) and during Heinrich Events (Vidal et al., 1997). However, other mechanisms have also been proposed to explain the Younger Dryas cold period, including changing atmospheric circulation (Wunsch, 2006; Brauer et al., 2008) and extraterrestrial impact (Firestone et al., 2007; Melott et al., 2010).

In addition to the 8.2 ka Event, other studies have presented evidence from oceanic sediment cores for meltwater-driven abrupt climatic events that may have perturbed deep ocean circulation patterns at 9.5 ka (Keigwin et al., 2004), 9.3 ka (Yu et al., 2010), 9.2 ka (Fleitmann et al., 2008, and references therein), 8.6 ka (Henderson, 2009), 8.4 ka (Kleiven et al., 2008), 4.2 ka (Booth et al., 2005; Menounos et al., 2008), 2.7 ka (Hall et al., 2004), and the Little Ice Age (1500–1900 AD; Bradley and Jones, 1993; Dahl-Jensen et al., 1998). While the evidence for these events has similarities in common with the sediment core records through the 8.2 ka Event and the Younger Dryas, they are less frequently observed in oceanic records and have yet to be directly tied to meltwater delivery routes.

Here, we present high-resolution proxy records of surface and deepwater environmental conditions from the northern North Atlantic to test the hypothesis that episodic surface water freshenings altered deepwater circulation patterns during the early Holocene. Records of proxies for surface water temperature (planktonic foraminiferal assemblage and $\delta^{18}O$ values), surface water stratification ($\Delta\delta^{18}O_{N.\ pachyderma\ (s)-G.\ bulloides}$, calculated from the difference between $\delta^{18}O_{G.\ bulloides}$ and $\delta^{18}O_{N.\ pachyderma\ (s)}$), ice rafted debris (IRD; quantity of lithic grains/g), bottom water temperature ($\delta^{18}O$ benthic foraminifera), and deep ocean circulation ($\delta^{13}C$ benthic foraminifera) are used to compare surface water hydrography with NADW variations during the critical Holocene interval.

2. Methods

2.1. Site information and sample processing

Surface ocean currents bring warm, salty surface water to the northeast North Atlantic via the North Atlantic Current, which bifurcates toward western Europe and the Nordic Seas, passing between the North Atlantic subpolar and subtropical gyres (Fig. 1; Hansen and Østerhus, 2000). The surface waters cool and sink in the Nordic Seas, returning to the North Atlantic as Iceland–Scotland Overflow Water (ISOW) and Denmark Strait Overflow Water (DSOW; Worthington, 1976; Fig. 1). The contributions of ISOW and DSOW are related to surface temperature and salinity in the Nordic Seas (Duplessy et al., 1988), as well as to surface inflow (Thornalley et al., 2009) controlled by the position and strength of North Atlantic gyres (Hansen and Østerhus, 2000), sill depth (Millo et al., 2006), sea ice cover (Prins et al., 2001; Raymo et al., 2004), and tectonics (Wright and Miller, 1996). Thus, researchers have suggested that overflow strength has varied on geologic, orbital, decadal and inter-annual timescales (Duplessy eat al., 1988; Oppo et al., 1995; Dokken and Hald, 1996; Wright and Miller, 1996; Bianchi and McCave, 1999; McManus et al., 1999; Turrell et al., 1999; Dickson et al., 2002; Raymo et al., 2004) Modern NADW is produced by the interplay between ISOW, DSOW, Antarctic Bottom Water (AABW), Labrador Sea Water, and Mediterranean Outflow Water (Mann, 1969; Worthington, 1976; Fig. 1). Due to their similar though complicated formation pathways, ISOW and DSOW export may co-vary or may have an inverse relationship (i.e. increased ISOW occurs at the expense of decreased DSOW); however this study has scope only to address the ISOW component.

Jumbo piston core 11JPC was collected by the *R/V Knorr* on cruise 166, leg 14, from 2707 m water depth on Gardar Drift (56°14′N, 27°39′W) in the eastern North Atlantic (Fig. 1; Table 1.). ISOW, the largest eastern source of modern North Atlantic Deepwater, bathes this site (Worthington, 1976; Bianchi and McCave, 1999). High sedimentation

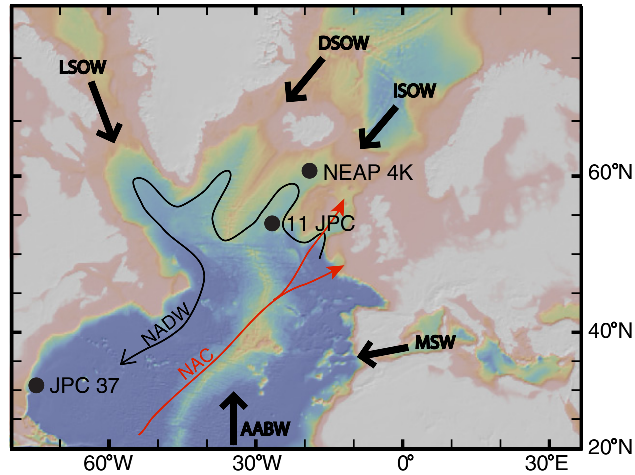

Fig. 1. Bathymetric map of the North Atlantic showing location of KN166-14 11JPC on Gardar Drift (this study), NEAP 4K (Hall et al., 2004), and KNR140-2 JPC 37 (Hagen and Keigwin, 2002). Generalized oceanographic currents are shown for surface flowing North Atlantic Current (NAC; red), and the five main contributors to North Atlantic Deep Water (NADW; black); Labrador Sea Overflow water (LSOW), Denmark Straits Overflow Water (DSOW), Iceland–Scotland Overflow Water (ISOW), Mediterranean Sea Water (MSW), and Antarctic Bottom Water (AABW).

rates (~18 cm/kyr) offer high temporal resolution throughout the Holocene (Fig. 2).

The top 222 cm of core 11JPC was sampled at 1 cm intervals to study changes in surface water hydrography during the Holocene and Younger Dryas, yielding a sampling resolution of ~58 years per sample (Elmore and Wright, 2011). The >150 μm fraction of each sample was split using a microsplitter into an aliquot containing at least 300 planktonic foraminifera (Imbrie and Kipp, 1971). Abundances of the planktonic foraminiferal species were determined by manual counting. The three most common taxa were left-coiling *Neogloboquadrina pachyderma* (sinestral; s), right-coiling *N. pachyderma* (dextral; d), and *Globogerina bulloides*. Planktonic foraminiferal assemblage results are reported as percent, with respect to the total planktonic foraminiferal assemblage. The polar biogeographic region is dominated by *N. pachyderma* (s), thus % *N. pachyderma* (s) has been used as an indicator of relative temperature changes for polar to subpolar regions (Bé and Tolderlund, 1971; Bé, 1977).

Up to 15 tests of each of the planktonic foraminifera species *N. pachyderma* (s) and *G. bulloides* were selected using a binocular microscope from the 250 to 350 μm size fraction of each sample and analyzed for stable isotopic composition on an Optima Mass Spectrometer at Rutgers University (1-σ laboratory precision of an internal lab standard was 0.08‰ for $\delta^{18}O$ and 0.05‰ for $\delta^{13}C$). The differences ($\Delta\delta^{18}O_{N.\ pachyderma\ (s)-G.\ bulloides}$) between the $\delta^{18}O$ values of the surface-dwelling *G. bulloides* and thermocline-dwelling *N. pachyderma* (s) were then calculated for each sample to determine the differences in calcification environment driven by the depth habitat preference of each species, as defined by Lagerklint and Wright (1999). Since these two species have been selected out of the same samples, global changes in $\delta^{18}O$ driven by ice volume and/or any regional changes in $\delta^{18}O_{sea\ water}$ would not affect the $\Delta\delta^{18}O$ difference as both species would record these effects contemporaneously (Lagerklint and Wright,

Table 1
Locations of sediment cores used in this study.

Site	Water depth (m)	Latitude	Longitude
KN166-14 11JPC	2707	56°15′N	27°40′W
NEAP 4K	1627	61°29.91′N	24°10.33′W
KNR140-2 JPC 37	3000	31°41′N	75°29′W

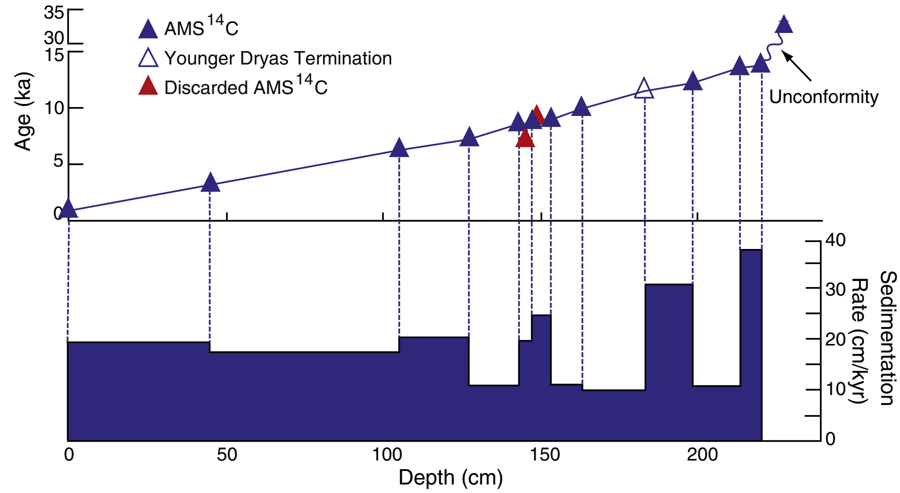

Fig. 2. Age model and sedimentation rate for core 11JPC, updated from Elmore and Wright (2011). The solid blue triangles represent AMS ^{14}C analyses used in generating the age model and red triangles represent discarded AMS ^{14}C analyses. The open blue triangle represents the chronostratigraphic tie point at the end of the Younger Dryas, which has been modified slightly from initial publication in Elmore and Wright (2011).

1999). In addition to having differing depth habitats, *N. pachyderma* (s) and *G. bulloides* may have seasonal preferences that could bias $\Delta\delta^{18}O_{N.\ pachyderma\ (s)-G.\ bulloides}$ values, however Fraile et al. (2009) demonstrate that both species used in this reconstruction preferentially reflect summer temperatures in the North Atlantic region. Additionally, the Greenland ice core $\delta^{18}O$ data do not show large-scale changes in seasonality throughout the Holocene (e.g., Steffensen et al., 2008), so any interspecies differences in the timing of calcification within the year are not expected to affect our multi-decadal time-averaged $\Delta\delta^{18}O_{N.\ pachyderma\ (s)-G.\ bulloides}$ record. Thus, the $\Delta\delta^{18}O_{N.\ pachyderma\ (s)-G.\ bulloides}$ difference between *N. pachyderma* (s) and *G. bulloides* is hereafter used to reflect variations in vertical stratification caused by fresh water inputs (Lagerklint and Wright, 1999; Pak and Kennett, 2002).

The number of lithic grains (>150 μm) per gram of dried sediment was counted as a proxy for ice-rafted detritus (IRD; Bond and Lotti, 1995). The location of 11JPC is too far from terrestrial sources to have a large quantity of lithic grains transported to the site by means other than ice rafting (e.g., Bond and Lotti, 1995).

Deepwater variations were reconstructed by measuring downcore benthic foraminiferal $\delta^{13}C$ values. Up to 5 tests of the benthic foraminifera *Planulina wuellerstorfi* were selected from the 250 to 350 μm size fraction and analyzed for stable oxygen and carbon isotopic composition (see above). Differences between the $\delta^{13}C$ value of bottom waters in the North Atlantic and the South Atlantic (~1‰ and ~0.4‰, respectively in the modern oceans; Kroopnick, 1980), which are recorded in epibenthic foraminifera, allow for the use of benthic foraminiferal $\delta^{13}C$ as a water mass tracer (e.g., Belanger et al., 1981; Graham et al., 1981). Only *P. wuellerstorfi* tests were chosen for analysis since some *Cibicidoides* taxa (e.g., *C. robertsonianus*) do not record equilibrium values and may be up to 1‰ lower in $\delta^{13}C$ values (Elmore, 2009). In addition to reflecting changes in water mass mixing, benthic foraminiferal $\delta^{13}C$ records can be complicated by changes in productivity and remineralization (Mackensen et al., 1993, 2001); these complicating factors are evaluated in the discussion section below.

2.2. Age model

Fifteen AMS ^{14}C ages constrain the age model for 11JPC (Fig. 2), which was previously presented in Elmore and Wright (2011). For each AMS ^{14}C analysis, 4–6 mg of planktonic foraminifera *G. bulloides* were selected using a binocular microscope and sonicated in deionized water. Samples were then analyzed at the Keck Center for Accelerator Mass Spectrometry at the University of California, Irvine. The resulting radiocarbon ages were converted to calendar ages according to the Fairbanks0805 calibration, after a standard 400-year reservoir correction was applied, which likely represents the minimum reservoir correction for the region (Fairbanks et al., 2005; Fig. 2). The Younger Dryas termination at 183 cm, as defined by % *N. pachyderma* (s) and $\delta^{18}O$ of *N. pachyderma* (s), was used as additional chrono-stratigraphic tie point (Alley et al., 1995; Ellison et al., 2006; Elmore and Wright, 2011) and defined as 11.7 ka (Walker et al., 2012); this represents a slight change from the original age model in Elmore and Wright (2011), wherein the end of the Younger Dryas was defined as 11.5 ka. AMS dates at 145 and 149 cm were not included in the age model because they produced slight age reversals (Fig. 2). According to the age model for 11JPC and the subdivisions of the Holocene Epoch according to Walker et al. (2012), the early Holocene (11.7–8.2 ka) is recorded in sediments from 183 to 141 cm; the middle Holocene (8.2–4.2 ka) is recorded in sediments from 140 to 72 cm; and the late Holocene (4.2 ka – present) is recorded in sediments from 71 to 0 cm (Fig. 2).

3. Results

3.1. Surface water results

The top 222 cm of the core is divided into two chronozones based on the age model (Fig. 2). The Younger Dryas (12.9–11.7 ka) section is from 222 to 184 cm, and is discussed in detail in Elmore and Wright (2011) and the Holocene section (11.7 ka – present) is from 183 cm to the top of the core (~0.7 ka). The Younger Dryas section of the core is dominated by polar planktonic foraminiferal species, *N. pachyderma* (s) (40–60%), and higher planktonic $\delta^{18}O_{N.\ pachyderma\ (s)}$ and $\delta^{18}O_{G.\ bulloides}$ values (2.0–3.5‰ and 2.0–2.5‰, respectively), indicating colder temperatures during the Younger Dryas than during the Holocene at 11JPC (Fig. 3A; B). The Younger Dryas to early Holocene changes in $\delta^{18}O_{N.\ pachyderma\ (s)}$ and $\delta^{18}O_{G.\ bulloides}$ values are ~1.4‰ and ~2.6‰, respectively; these changes cannot be solely explained by the change in $\delta^{18}O_{sea\ water}$ driven by continental ice volume since sea level rises less than 70 m through this interval (Peltier and Fairbanks, 2006), equating to a ~0.77‰ change in $\delta^{18}O_{sea\ water}$ according the relationship described by Shackelton (1974). While the residual change in $\delta^{18}O$ from the Younger Dryas to the Holocene, excluding ice volume effects, does include some localized salinity effects (supported by observed evidence for IRD during this interval), the general trends are too large to be accounted for by salinity changes alone, and therefore must represent some change in temperature.

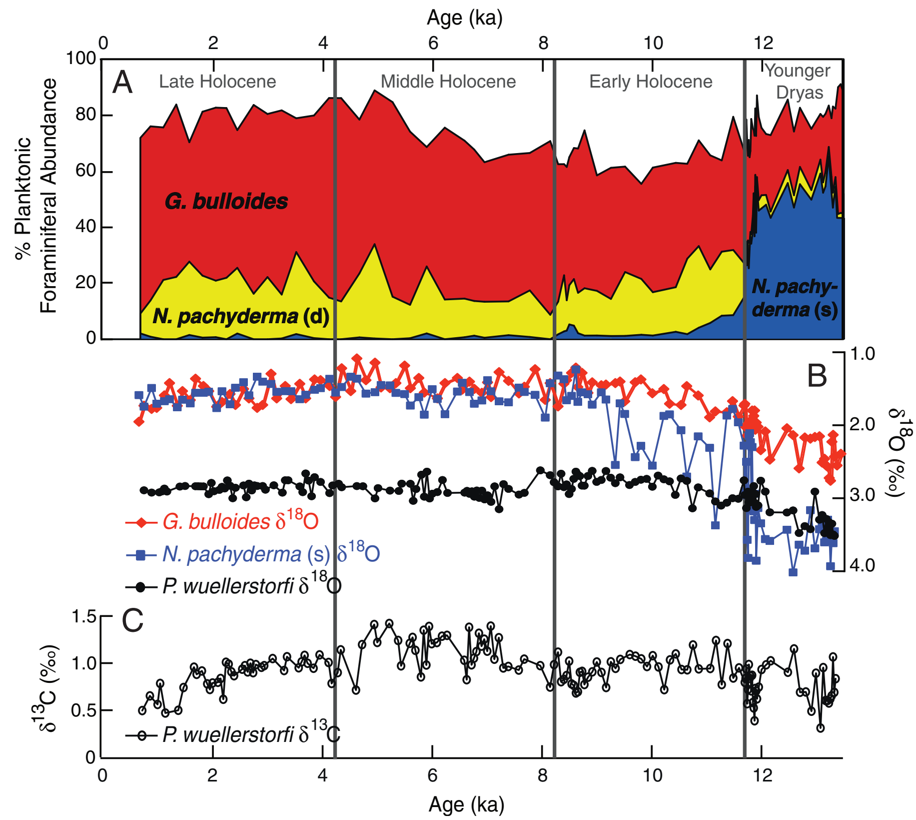

Fig. 3. Proxy records from core 11JPC plotted versus age from 0 to 13.5 ka, including; (A) planktonic foraminiferal abundances of major species, (B) $\delta^{18}O_{G.\ bulloides}$ (red diamonds), $\delta^{18}O_{N.\ pachyderma\ (s)}$ (blue squares), and $\delta^{18}O_{P.\ wuellerstorfi}$ (black circles), (C) $\delta^{13}C_{P.\ wuellerstorfi}$ (open black circles).

The early Holocene (~11.7–8.2 ka) section in core 11JPC is found between ~183 and 141 cm (Fig. 2). A decrease in % *N. pachyderma* (s) and a correspondingly large increase in % *G. bulloides* is observed in the early Holocene transitional section (Fig. 2), indicating a change from polar to subpolar conditions (Fig. 3A). *N. pachyderma* (s) $\delta^{18}O$ and $\delta^{18}O_{G.\ bulloides}$ values also decrease across this transitional section (Fig. 3B). Superimposed on the decreasing trend of the early Holocene, abrupt and episodic changes in $\delta^{18}O_{N.\ pachyderma\ (s)}$ are an obvious feature of the record (Fig. 3B). Lithic grain abundances decrease abruptly across the Younger Dryas–Holocene boundary (~11.7 ka) but some lithic grain inputs are continually observed throughout the early Holocene (Fig. 4D).

In the middle Holocene (8.2–4.2 ka), the abundance of the polar species, *N. pachyderma* (s) is typically less than 3% (Fig. 3A). The abundances of sub-polar species *G. bulloides* and right coiling *N. pachyderma* (d) are ~50% and ~20%, respectively, indicating that the sub-polar waters gradually replaced the polar conditions of the Younger Dryas during the early Holocene chronozone (Fig. 3A). This foraminiferal abundance shift ushered in the modern assemblage, which persisted throughout the remainder of the Holocene (Fig. 3A). *N. pachyderma* (s) $\delta^{18}O$ values decrease from ~2.8 to 1.7‰ in the early Holocene chronozone and are low (~1.7–1.4‰), with limited variability, in the middle and late Holocene section (Fig. 3B). *G. bulloides* $\delta^{18}O$ values are also low and steady (~1.2–1.8‰) throughout the Holocene chronozone, indicating relatively warm surface temperatures (Fig. 3B). The abundance of lithic grains per gram is low overall in the middle and late Holocene, with an average value of 8 grains/g, but small, episodic peaks are recorded (Fig. 4D).

3.2. Deepwater results

Deepwater temperature and circulation proxies show variations between Younger Dryas and Holocene conditions at site 11JPC (Fig. 3). Benthic foraminiferal $\delta^{18}O$ decreases from ~3.5 to 2.9‰ through the Younger Dryas and early Holocene sections, similar to the expected global signature from ice volume change outlined above, indicating that bottomwater did not warm significantly through the interval (Fig. 3C). Similarly, $\delta^{18}O_{P.\ wuellerstorfi}$ values remain fairly constant through the Holocene section, indicating a stable deep ocean temperature, without higher frequency variations (Fig. 3C).

The Younger Dryas chronozone is typified by low $\delta^{13}C_{P.\ wuellerstorfi}$ values at the beginning and end of the chronozone, with distinct abrupt minima of ~0.4‰ (Fig. 3C; Elmore and Wright, 2011). *P. wuellerstorfi* $\delta^{13}C$ values increase generally through the early Holocene chronozone, to a mid-Holocene maxima value of ~1.3‰ at ~7.0 ka. Short-lived minima in $\delta^{13}C_{P.\ wuellerstorfi}$ are superimposed on this early Holocene increase, with values ~0.6‰, suggesting abrupt circulation changes in the North Atlantic (Figs. 3C; 4E). A long-term decreasing trend in $\delta^{13}C_{P.\ wuellerstorfi}$ values is then observed from ~5 ka to the top of the record at ~0.7 ka, without abrupt variations (Figs. 3C;4E).

4. Discussion

The early Holocene section of core 11JPC is typified by generally decreasing values of $\delta^{18}O_{G.\ bulloides}$, $\delta^{18}O_{N.\ pachyderma\ (s)}$, $\delta^{18}O_{P.\ wuellerstorfi}$, and decreasing % *N. pachyderma* (s), all of which indicate a warming trend from 11.7 to 8.2 ka (Fig. 3A; B; C). Early Holocene $\Delta\delta^{18}O_{N.\ pachyderma\ (s)–G.\ bulloides}$ values also show a generalized decreasing trend, with numerous abrupt variations (to <0.5‰; Fig. 4C), indicating episodic increases in upper ocean stratification driven by meltwater, overlying a trend toward decreasing stratification into the mid-Holocene. Lithics per gram show a general decrease through the early Holocene (to <10 lithics/g; Fig. 4D), indicating that some proximal IRD occurred throughout the warming period of the early Holocene, but disappeared by the mid-Holocene. Interestingly, the IRD record (Fig. 4D)

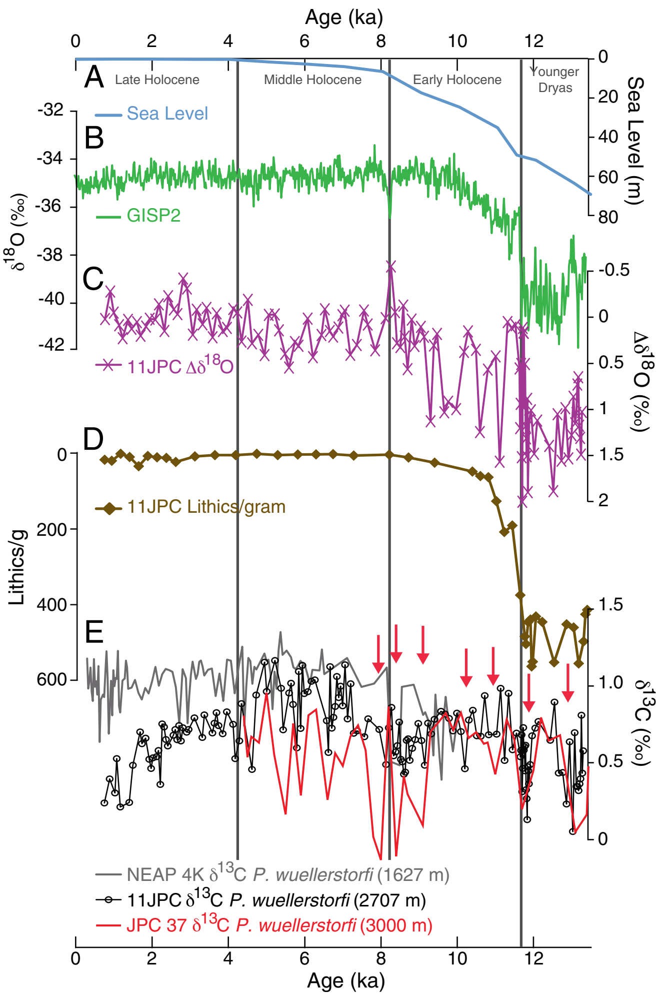

Fig. 4. Proxy records from core 11JPC shown versus age from 13.5 ka to present plotted with (A) generalized sea level record for post-deglaciation (blue; after Peltier and Fairbanks, 2006), (B) the $\delta^{18}O$ record from Greenland ice core, GISP2 (green; Stuiver et al., 1995), (C) 11JPC $\Delta\delta^{18}O_{G.\ bulloides-N.\ pachyderma\ (s)}$ (purple x), (D) 11JPC Lithics/g (brown diamonds), (E) 11JPC $\delta^{13}C_{P.\ wuellerstorfi}$ (black open circles), NEAP 4K $\delta^{13}C_{P.\ wuellerstorfi}$ (gray; Hall et al., 2004), and JPC37 $\delta^{13}C_{P.\ wuellerstorfi}$ (red; Hagen and Keigwin, 2002). The vertical red arrows signify times of decreased $\delta^{13}C_{P.\ wuellerstorfi}$ at 11JPC, suggesting more southern-sourced waters due to decreased northern-sourced deep water formation.

does not seem to show the episodic variations of $\Delta\delta^{18}O_{N.\ pachyderma\ (s)-G.\ bulloides}$ (Fig. 4C), which is driven by the large changes in $\delta^{18}O_{N.\ pachyderma\ (s)}$ (Fig. 3B). This is likely due in part to the coarser sampling interval for IRD counting (for example, no IRD data points exist ~9.6 ka). Additionally, not all meltwater is associated with IRD, and meltwater may have a wider geographic effect than debris carried by ice rafting.

Values of $\delta^{13}C_{P.\ wuellerstorfi}$ from 11JPC also show high variability superimposed on a general increasing trend through the early Holocene; lows in $\delta^{13}C_{P.\ wuellerstorfi}$ are highlighted by red arrows in Fig. 4E and are larger than the analytical uncertainty of 0.05‰. If the $\delta^{13}C_{P.\ wuellerstorfi}$ are interpreted to represent variable contributions of northern versus southern sources of deep water (e.g., Curry and Oppo, 2005), the data from 11JPC suggest that abrupt circulation changes occurred within a longer-term increase in the export of northern-sourced water (Fig. 4E). Similar trends in variable early Holocene benthic foraminiferal $\delta^{13}C$ can also be seen from sites around the North Atlantic, including at Blake Outer Ridge (JPC37; Hagen and Keigwin, 2002; Evans and Hall, 2008; Figs. 1; 4E; Table 1). Air–sea exchange, preformed nutrients, and localized micro-environments (Mackensen et al., 1993) may complicate interpretations of benthic foraminiferal $\delta^{13}C$ in terms of circulation changes, however, benthic foraminiferal $\delta^{13}C$ has been routinely interpreted to reflect circulation in this region (e.g., Hall et al., 2004; Thornalley et al., 2009, 2010; Elmore and Wright, 2011; Hoogakker et al., 2011), supporting our use of $\delta^{13}C_{P.\ wuellerstorfi}$ as a watermass tracer. Additionally, our interpretations of circulation changes are consistent with reconstructions using sortable silt grain size, an inorganic proxy for flow speed, which also shows abrupt variations in circulation during the early Holocene (Bianchi and McCave, 1999; Hoogakker et al., 2011). The observed changes in $\delta^{13}C_{P.\ wuellerstorfi}$ from 11JPC cannot be explained by changes in source region, since records of $\delta^{13}C$ from sites bathed by Norwegian Sea Deep Water, a formation region for ISOW, do not show similarities in trend with 11JPC or other records from the Northeast North Atlantic (e.g., Hoogakker et al., 2011; Hall et al., 2004; Fig. 4E). As shown in Fig. 4E, the shallower site NEAP 4K (Hall et al., 2004) records $\delta^{13}C_{P.\ wuellerstorfi}$ values that are equal to or higher than 11JPC $\delta^{13}C_{P.\ wuellerstorfi}$ through the entire interval 10–0 ka, with the exception of the lowest point in the NEAP 4K record at ~9.6 ka; this indicates that the Northern Source end member, ISOW, is not driving the decreases in $\delta^{13}C_{P.\ wuellerstorfi}$ at 11JPC. Rather, episodic decreases in $\delta^{13}C_{P.\ wuellerstorfi}$ at 11JPC record values that are more similar to down-stream NADW site JPC37 (Hagen and Keigwin, 2002), suggesting a greater southern source influence on benthic $\delta^{13}C$ during these episodic periods from 13 to 8 ka (Fig. 4E).

Early Holocene episodic meltwater pulses (Seidenkrantz et al., 2013) coincident with NADW circulation fluctuations can be explained by the residual melting of northern hemisphere ice sheets, which contributed to the ~30 m sea level rise during the early Holocene (Peltier and Fairbanks, 2006; Fig. 4A). The final collapse of the Northern Hemisphere ice sheets would have subsequently provided fresh meltwater to the surface of the North Atlantic, which could have then changed the density of NADW, affecting the depth to which this water mass penetrated. This is consistent with the idea that early Holocene was an unstable period and that the full interglacial period began well after 9 ka, coincident with the maximum flux of NADW (Henderson, 2009).

Climate events at 8.2 ka (Alley et al., 1997; Rohling and Pälike, 2005; Hald et al., 2007), 8.4 ka (Kleiven et al., 2008), and 8.6 ka (Henderson, 2009) have all been attributed to freshwater pulse(s) from Glacial Lake Agassiz, and proposed to have altered deepwater circulation patterns (Kleiven et al., 2008; Henderson, 2009); given the uncertainties in individual chronologies, these 'events' could all be part of the same meltwater event or could represent a series of meltwater events. The record of % *N. pachyderma* from 11JPC suggests a slight cooling ~8.4 ka; however, the cooling is not seen in records of $\delta^{18}O$ of *G. bulloides* or *N. pachyderma* (s; Fig. 4). It is possible that the sample resolution of 11JPC does not allow us to resolve the short-lived 8.2 ka Event. The $\Delta\delta^{18}O_{N.\ pachyderma\ (s)-G.\ bulloides}$ values are higher during the period from 9 to 8 ka, indicating an increase in meltwater occurrence during that interval (Fig. 4C). During the period from 9 to 8.2 ka, the record of $\delta^{13}C_{P.\ wuellerstorfi}$ has several minima that could be perceived to represent abrupt changes in circulation, however $\delta^{13}C_{P.\ wuellerstorfi}$ values are generally low during the period from 9 to 8.2 ka, and thus it is difficult to decipher individual events from variability within the record (Fig. 4E).

The mid-Holocene, from ~8.2 to 4.2 ka, is characterized by slightly warmer surface temperatures according to records of $\delta^{18}O_{G.\ bulloides}$ and $\delta^{18}O_{N.\ pachyderma\ (s)}$ (Fig. 3B). The lithics per gram and $\Delta\delta^{18}O_{N.\ pachyderma\ (s)-G.\ bulloides}$ values approach 0 during this time, indicating minimal seasonal and/or stratification differences, and thus no apparent meltwater (Fig. 4C; D). Values of $\delta^{13}C_{P.\ wuellerstorfi}$ from 11JPC are high, suggesting a maximum northern-sourced component to deepwater flow (Fig. 3C). From 8 to 4 ka, benthic foraminiferal $\delta^{13}C$ values from the ISOW-proximal sites NEAP 4K and 11JPC are very similar, with a variable gradient between the ISOW-proximal sites and the downstream NADW site (JPC37; Fig. 4E), suggesting either changes in the downstream processes forming NADW (possibly a changed input of DSOW or LSW) or southern intrusion to the downstream site, JPC37. This indicates that the warmest period of the Holocene, including the Holocene Thermal Maximum, was a period of vigorous deepwater flow, consistent with previous research (Davis, 1984; Davis et al., 2003; Kaufman et al., 2004; Henderson, 2009).

During the late Holocene, from 4.2 ka to present, sea surface temperatures remain warm, indicated by low $\delta^{18}O_{G.\ bulloides}$ and $\delta^{18}O_{N.\ pachyderma\ (s)}$ (Fig. 3B) and high % *G. bulloides* (Fig. 3A); similar to the reconstructions by Andersson et al. (2010) from surface and near surface foraminiferal geochemistry. Low lithics/g and low $\Delta\delta^{18}O_{N.\ pachyderma\ (s)–G.\ bulloides}$ indicate that there was very little meltwater present during the late Holocene (Fig. 4C; D). Interestingly, the *P. wuellerstorfi* $\delta^{13}C$ values at 11JPC decrease, especially from ~2.0 to 0.6 ka, which could indicate a change in deepwater circulation or a change in preformed nutrients (Fig. 4E). If interpreted in terms of circulation, the divergence between $\delta^{13}C_{P.\ wuellerstorfi}$ 11JPC and ISOW-proximal NEAP 4K in the late Holocene suggests that the 11JPC record is controlled by southern-sourced water rather than responding to northern-derived source water changes (Fig. 4E). However, this interpretation seems at odds with $\delta^{13}C_{P.\ wuellerstorfi}$ results from shallower northern cores under the influence of ISOW (IODP 984 and NEAP 4K; Praetorius et al., 2008; Hall et al., 2004) and sortible silt flow speed records (NEAP 15K; Bianchi and McCave, 1999), all of which indicate vigorous ISOW formation throughout the late Holocene. Thus, it may simply indicate that the latest Holocene benthic foraminiferal $\delta^{13}C$ record is controlled by local sources, rather than large scale circulation changes, including the possibility of late Holocene organic input changes (e.g., Mackensen et al., 1993).

Taken holistically, these records indicate that, while there is evidence for continued meltwater in the region of 11JPC from the Younger Dryas (Elmore and Wright, 2011) through the early Holocene, the NADW circulation changes through this interval are episodic, rather than continual. This suggests that the rate of meltwater delivery and/or the location of meltwater delivery are important factors in determining the impact on NADW circulation resulting from meltwater input in to the North Atlantic (Fanning and Weaver, 1997; Elmore and Wright, 2011).

5. Conclusions

High-resolution records from the southern Gardar Drift show evidence for multiple meltwater events and associated deepwater circulation perturbations during the early Holocene. The $\Delta\delta^{18}O_{N.\ pachyderma\ (s)–G.\ bulloides}$ and lithic/g evidence for meltwater delivery to the North Atlantic during the early Holocene coincides with benthic foraminiferal $\delta^{13}C_{P.\ wuellerstorfi}$ evidence for multiple changes in deepwater circulation. This linkage indicates that abrupt releases of meltwater from the Laurentide (via eastern or Arctic pathways) and/or Fenno-Scandinavian Ice Sheets directly forced deepwater circulation changes in the North Atlantic during the early Holocene. Lower surface salinities throughout the North Atlantic region inhibited deep convection in the northern North Atlantic, which led to multiple early Holocene decreases in benthic foraminiferal $\delta^{13}C_{P.\ wuellerstorfi}$ values. Circulation fully recovered during the mid-Holocene, when all residual glacial sea-level rise was completed, and as sea surface temperatures reached a maximum. This study provides a direct link between surface water freshening and alterations in deepwater circulation patterns during the early Holocene. However, by and large, the freshwater contribution to the northern North Atlantic during the early Holocene interval had very little influence on large-scale climate, with the possible exception of the 8.2 kyr Event.

Acknowledgments

We would like to thank E. McClymont, J. McManus, K. Miller, G. Mountain, D. Thornalley, L. Neitzke, S. Henderson, R. Mortlock, and Y. Rosenthal for their helpful discussions and comments on earlier versions of this manuscript, and Kraig Wray for analytical assistance. The comments from the Editor, Gert De Lange, and 2 anonymous reviewers greatly improved this manuscript. This research was supported by the National Science Foundation grant OCE-0095219 to J. D. Wright. Data from this study has been archived at *http://www.ncdc.noaa.gov/paleo/study/17536*.

References

Alley, R.B., Gow, A.J., Johnsen, S.J., Kipfstuhl, J., Messe, D.A., Thorsteinsson, T., 1995. Comparison of deep ice cores. Nature 373, 393–394.
Alley, R.B., Mayewski, P.A., Sowers, T., Stuiver, M., Taylor, K.C., Clark, P.U., 1997. Holocene climatic instability: a prominent, widespread event 8200 yr ago. Geology 25 (6), 483–486.
Andersson, C., Pausata, F.S.R., Jansen, E., Risebrobakken, B., Telford, R.J., 2010. Holocene trends in the foraminifer record from the Norwegian Sea and the North Atlantic Ocean. Climate of the Past 6, 179–193.
Andrews, J.T., Dunhill, G., 2004. Early to mid-Holocene Atlantic water influx and deglacial events, Beaufort Sea slope, Arctic Ocean. Quaternary Research 61, 14–21.
Atkinson, T.C., Briffa, K.R., Coope, G.R., 1987. Seasonal temperatures in Britain during the past 22,000 years, reconstructed using beetle remains. Nature 325, 587–592.
Barber, D.C., Dyke, A., Hillaire-Marcel, C., Jennings, A.E., Andrews, J.T., Kerwin, M.W., Bilodeau, G., McNeely, R., Southon, J., More-head, M.D., Gagnon, J.-M., 1999. Nature 400, 344–348.
Bard, E., Hamelin, B., Delanghe-Sabatier, D., 2010. Deglacial meltwater Pulse 1B and Younger Dryas sea levels revisited with boreholes at Tahiti. Science 327, 1235–1237.
Bé, A.W.H., 1977. An ecological, zoogeographic and taxonomic review of recent planktonic foraminifera. In: Ramsay, A.T.S. (Ed.), Oceanic Micropaleontology 1. Academic Press, London, pp. 1–100.
Bé, A.W.H., Tolderlund, D.S., 1971. Distribution and ecology of living planktonic foraminifera in surface waters of the Atlantic and Indian Oceans. In: Funnel, B.M., Riedel, W.R. (Eds.), The Micropaleontology of Oceans, pp. 105–149.
Belanger, P.E., Curry, W.B., Matthews, R.K., 1981. Core top evaluation of benthic foraminiferal isotopic ratios for paleoceanographic interpretations. Palaeoceanography, Palaeoclimatology, Palaeoecology 33, 205–220.
Bianchi, G.G., McCave, N., 1999. Holocene periodicity in North Atlantic climate and deep-ocean flow south of Iceland. Nature 397, 515–517.
Bond, G.C., Lotti, R., 1995. Iceberg discharges into the North Atlantic on millennial time scales during the Last Glaciation. Science 267, 1005–1010.
Bond, G.C., Showers, W., Cheseby, M., Lotti, R., Almasi, P., deMenocal, P., Priore, P., Cullen, H., Hajdas, I., Bonani, G., 1997. A pervasive millennial-scale cycle in North Atlantic Holocene and Glacial climates. Science 278, 1257–1267.
Booth, R.K., Jackson, S.T., Forman, S.L., Kutzbach, J.E., Bettis, E.A., Kreigs, J., Wright, D.K., 2005. A severe centennial-scale drought in midcontinental North America 4200 years ago and apparent global linkages. The Holocene 15 (3), 321–328.
Born, A., Levermann, A., 2010. The 8.2 ka event: abrupt transition of the subpolar gyre toward a modern North Atlantic circulation. Geochemistry, Geophysics, Geosystems 11 (6).
Bradley, R.S., Jonest, P.D., 1993. 'Little Ice Age' summer temperature variations: their nature and relevance to recent global warming trends. The Holocene 3, 367–376.
Brauer, A., Haug, G.H., Dulski, P., Sigman, D.M., Negendank, J.F.W., 2008. An abrupt wind shift in western Europe at the onset of the Younger Dryas cold period. Nature Geoscience 1, 520–523.
Broecker, W.S., Kennett, J.P., Flower, B.P., Teller, J.T., Trumbore, S., Bonani, G., Wolfi, W., 1989. Routing of meltwater from the Laurentide Ice Sheet during the Younger Dryas cold episode. Nature 341, 318–321.
Clark, P.U., Marshall, S.J., Clarke, G.K.C., Hostetler, S.W., Licciardi, J.M., Teller, J.T., 2001. Freshwater forcing of abrupt climate change during the Last Glaciation. Science 293, 283–287.
Cronin, T.M., Vogt, P.R., Willard, D.A., Thunell, R., Halka, J., Berke, M., Pohlman, J., 2007. Rapid sea level rise and ice sheet response to 8200-year climate event. Geophysical Research Letters 34 (20).
Curry, W.B., Oppo, D.W., 2005. Glacial water mass geometry and the distribution of $\delta^{13}C$ and $\sum CO_2$ in the western Atlantic Ocean. Paleoceanography 20, 1–12.
Dahl-Jensen, D., Mosegard, K., Gundestrup, N., Clow, G.D., Johnsen, S.J., Hansen, A.W., Balling, N., 1998. Past temperatures directly from the Greenland ice sheet. Science 282, 268–271.
Dansgaard, W., Johnsen, S.J., Clausen, H.B., Dahl-Jensen, D., Gundestrup, N., Hammer, C.U., Oeschger, H., 2014. North atlantic climate oscillations revealed by deep greenland ice cores. Climate Process and Climate Sensitivity. http://dx.doi.org/10.1029/GM029p0288 (in press).
Davis, O.K., 1984. Multiple Thermal Maximum during the Holocene. Science 225, 617–619.
Davis, B.A.S., Brewer, S., Stevenson, A.C., Guiot, J., Contributors, Data, 2003. The temperature of Europe during the Holocene reconstructed from pollen data. Quaternary Science Reviews 22, 1701–1716.
Deschamps, P., Durand, N., Bard, E., Hamelin, B., Camoin, G., Thomas, A.L., Henderson, G.M., Okuno, J., Yokoyama, Y., 2012. Ice-sheet collapse and sea-level rise at the Bolling warming 14,600 years ago. Nature 483, 559–564.
Dickson, B., Yashayaev, I., Meincke, J., Turrell, B., Dye, S., Holfort, J., 2002. Rapid freshening of the deep North Atlantic Ocean over the past four decades. Nature 416, 832–837.
Dokken, T., Hald, M., 1996. Rapid climatic shifts during isotopes stages 2–4 in the Polar North Atlantic. Geology 24 (7), 599–602.

Duplessy, J.C., Shackleton, N.J., Fairbanks, R.G., Labeyrie, L., Oppo, D.W., Kallel, N., 1988. Deepwater source variations during the last climatic cycle and their impact on the global deep-water circulation. Paleoceanography 3 (3), 342–360.

Ellison, C.R.W., Chapman, M.R., Hall, I.R., 2006. Surface and deep ocean interactions during the cold climate event 8200 years ago. Science 312, 1929–1933.

Elmore, A.C., 2009. Late Pleistocene changes in northern component water: inferences from geochemical and sedimentological records from Gardar Drift. (Ph.D. Dissertation), Rutgers University (225 pages).

Elmore, A.C., Wright, J.D., 2011. North Atlantic Deep Water and climate variability during the Younger Dryas cold period. Geology 41, 1251–1254.

Evans, H.K., Hall, I.R., 2008. Deepwater circulation on Blake Outer Ridge (western North Atlantic) during the Holocene, Younger Dryas, and Last Glacial Maximum. Geochemistry, Geophysics, Geosystems 9 (3), 1–19.

Fairbanks, R.G., 1989. A 17,000-year glacio-eustatic sea level record: influence of glacial melting rates on the Younger Dryas event and deep-ocean circulation. Nature 342, 637–642.

Fairbanks, R.G., Mortlock, R.A., Chiu, T.-C., Cao, L., Kaplan, A., Guilderson, T.P., Fairbanks, T.W., Bloom, A.L., 2005. Marine radiocarbon calibration curve spanning 0 to 50,000 years B.P. Based on paired $^{230}Th/^{234}U/^{238}U$ and ^{14}C dates on pristine corals. Quaternary Science Reviews 24, 1781–1796.

Fanning, A.F., Weaver, A.J., 1997. Temporal–geographical meltwater influences on the North Atlantic Conveyor: implications for the Younger Dryas. Paleoceanography 12 (2), 307–320.

Firestone, R.B., et al., 2007. Evidence for an extraterrestrial impact 12,900 years ago that contributed to the megafaunal extinctions and the Younger Dryas cooling. PNAS 104 (41), 16016–16021.

Fleitmann, D., Mudelsee, M., Burns, S.J., Bradley, R.S., Kramers, J., Matter, A., 2008. Evidence for a widespread climatic anomaly at around 9.2 ka before present. Paleoceanography 23.

Fraile, I., Mulitza, S., Schulz, M., 2009. Modeling planktonic foraminiferal seasonality: implications for sea-surface temperature reconstructions. Marine Micropaleontology 72 (1–2), 1–9.

Graham, D.W., Corliss, B.H., Bender, M.L., Keigwin, L.D., 1981. Carbon and oxygen isotopic disequilibria of recent deep-sea benthic foraminifera. Marine Micropaleontology 6, 483-479.

Grootes, P.M., Stuiver, M., White, J.W.C., Johnsen, S., Jouzel, J., 1993. Comparison of oxygen isotope records from the GISP2 and GRIP Greenland ice cores. Nature 366, 552–554.

Hagen, S., Keigwin, L.D., 2002. Sea-surface temperature variability and deep water reorganisation in the subtropical North Atlantic during Isotope Stage 2–4. Marine Geology 189 (1–2), 145–162.

Hald, M., Andersson, C., Ebbesen, H., Jansen, E., Klitgaard-Kristensen, D., Risebrobakken, B., Salomonsen, G., Sarnthein, M., Sejrup, H.P., Telfod, R., 2007. Variations in temperature and extent of Atlantic Water in the northern North Atlantic during the Holocene. Quaternary Science Reviews 26 (25–28), 3423–3440.

Hall, I.R., Bianchi, G.G., Evans, J.R., 2004. Centennial to millennial scale Holocene climate-deep water linkage in the North Atlantic. Quaternary Science Reviews 23 (14–15), 1529–1536.

Hansen, B., Østerhus, S., 2000. North Atlantic–Nordic Seas exchanges. Progress in Oceanography 45, 109–208.

Henderson, S.S., 2009. Tracking deep-water flow on Eirik Drift over the past 160 kyr: linking deep-water changes to freshwater fluxes. (Ph.D. Dissertation), Rutgers University (160 pages).

Hillaire-Marcel, C., de Vernal, A., Piper, J.W., 2007. Lake Agassiz final drainage event in the northwest North Atlantic. Geophysical Research Letters 34 (15) L15601.

Hoogakker, B.A.A., Chapman, M.R., McCave, I.N., Hillaire-Marcel, C., Ellison, C.R.W., Hall, I.R., Telford, R.J., 2011. Dynamics of North Atlantic Deep Water masses during the Holocene. Paleoceanography 26, PA4214.

Imbrie, J., Kipp, N.G., 1971. A new micropaleontological method for quantitative paleoclimatology: application to a late Pleistocene Caribbean Core. In: Turekian, K.K. (Ed.), The Late Cenozoic Glacial Ages. Yale Univ. Press, New Haven, CT, pp. 71–181.

Kaufman, D.S., Ager, T.A., Anderson, N.J., Anderson, P.M., Andrews, J.T., Bartlein, P.J., Brubaker, L.B., Coats, L.L., Cwynar, L.C., Duvall, M.L., Dyke, A.S., Edwards, M.E., Eisner, W.R., Gajewski, K., Geirsdottir, A., Hu, F.S., Jennings, A.E., Kaplan, M.R., Kerwin, M.W., Lozhkin, A.V., MacDonald, G.M., Miller, G.H., Mock, C.J., Oswalt, W.W., Oppt-Cliesner, B.L., Porinchu, D.F., Ruhland, K., Smol, J.P., Steig, E.J., Wolf, B.B., 2004. Holocene thermal maximum in the western Arctic (0–180 W). Quaternary Science Reviews 23, 519–560.

Keigwin, L.D., 2004. Radiocarbon and stable isotope constraints on Last Glacial Maximum and Younger Dryas ventilation in the western North Atlantic. Paleoceanography 19, 1–15.

Kleiven, H.F., Kissel, C., Laj, C., Ninnemann, U.S., Richter, T.O., Cortijo, E., 2008. Reduced North Atlantic deepwater coeval with the Glacial Lake Agassiz fresh water outburst. Science 319, 60–65.

Kroopnick, P., 1980. The distribution of ^{13}C in the Atlantic Ocean. Earth and Planetary Science Letters 49, 469–484.

Lagerklint, I.M., Wright, J.D., 1999. Late glacial warming prior to Heinrich event 1: the influence of ice rafting and large ice sheets on the timing of initial warming. Geology 27 (12), 1099–1102.

Larsen, D.J., Miller, G.H., Geirsdottir, A., Olafsdottir, S., 2012. Non-linear Holocene climate evolution in the North Atlantic: a high-resolution, multi-proxy record of glacier activity and environmental change from Hvitarvatn, central Iceland. Quaternary Science Reviews 39, 14–25.

Liu, Y.-H., Henderson, G., Hu, C.-Y., Mason, A.J., Charnley, N., Johnson, K.R., Xie, S.-C., 2013. Links between the East Asian monsoon and North Atlantic climate during the 8200 year event. Nature Geoscience 6, 117–120.

Mackensen, A., et al., 1993. The $\delta^{13}C$ in benthic foraminiferal tests of *Fontbotia wuellerstorfi* (Schwager) relative to the $\delta^{13}C$ of dissolved inorganic carbon in Southern Ocean deep water: implications for glacial ocean circulation models. Paleoceanography 8, 587–610.

Mackensen, A., et al., 2001. Late Pleistocene deep-water circulation in the sub-Antarctic eastern Atlantic. Global and Planetary Change 30, 197–229.

Mann, C.R., 1969. Temperature and salinity characteristics of the Denmark Strait overflow. Deep-Sea Research 16, 125–137.

Marcott, S.A., Shakun, J.D., Clark, P.U., Miz, A.C., 2013. A reconstruction of regional and global temperature for the past 11,300 years. Science 339 (6124), 1198–1201.

McManus, J.F., Oppo, D.W., Cullen, J.L., 1999. A 0.5-million-year record of millennial-scale climate variability in the North Atlantic. Science 283, 971–975.

McManus, J.F., Francois, R., Gherardi, J.-M., Keigwin, L.D., Brown-Leger, S., 2004. Collapse and rapid resumption of Atlantic meridional circulation linked to deglacial climate changes. Nature 428, 834–837.

Melott, A.L., Thomas, B.C., Dreschhoff, G., Johnson, C.K., C.K., 2010. Cometary airbursts and atmospheric chemistry: Tunguska and a candidate Younger Dryas event. Geology 38, 355–358.

Menounos, B., Clague, J.J., Osborn, G., Luckman, B.H., Lakeman, T.R., Minkus, R., 2008. Western Canadian glaciers advance in concert with climate change circa 4.2 ka. Geophysical Research Letters 35 (7).

Miller, K.R., Chapman, M.R., 2013. Holocene climate variability reflected in diatom-derived sea surface temperature records from the subpolar North Atlantic. The Holocene 23, 882.

Millo, C., Sarnthein, M., Voelker, A., Erienkeuser, H., 2006. Variability of the Denmark strait overflow during the Last Glacial Maximum. Boreas 1, 50–60.

Oppo, D.W., Raymo, M.E., Lohmann, G.P., Mix, A.C., Wright, J.D., Prell, W.L., 1995. A $\delta^{13}C$ record of Upper North Atlantic Deep Water during the past 2.6 million years. Paleoceanography 10 (3), 373–394.

Pak, D.K., Kennett, J.P., 2002. A foraminiferal isotopic proxy for upper water mass stratification. Journal of Foraminiferal Research 32 (3), 319–327.

Peltier, W.R., Fairbanks, R.G., 2006. Global glacial ice volume and Last Glacial Maximum duration from an extended Barbados sea level record. Quaternary Science Reviews 25, 3322–3337.

Praetorius, S.K., McManus, J.F., Oppo, D.W., Curry, W.B., 2008. Episodic reductions in bottom-water currents since the last ice age. Nature Geoscience 1, 449–452.

Prins, M.A., Troelstra, S.R., Kruk, R.W., van der Borg, K., de Jong, A.F.M., Weltje, G.J., 2001. The Late Quaternary sediment record of the Reykjanes Ridge, North Atlantic. Radiocarbon 43 (2B), 939–947.

Raymo, M.E., Oppo, D.W., Flower, B.P., Flower, Hodell, D.A., McManus, J.F., Venz, K.A., Kleiven, K.F., McIntyre, K., 2004. Stability of North Atlantic water masses in face of pronounced climate variability during the Pleistocene. Paleoceanography 19, 1–13.

Renssen, H., Goosse, H., Fichefet, T., Campin, J.-M., 2001. The 8.2 kyr BP event simulated by a global atmosphere–sea–ice–ocean model. Geophysical Research Letters 28 (8), 1567–1570.

Renssen, H., Seppa, H., Crosta, X., Goosse, H., Roche, D.M., 2012. Global characterization of the Holocene Thermal Maximum. Quaternary Science Reviews 48, 7–19.

Rohling, E.J., Pälike, H., 2005. Centennial-scale climate cooling with a sudden cold even around 8200 years ago. Nature 434, 975–979.

Seidenkrantz, M.-S., Ebbesen, H., Aagaard-Sorensen, S., Moros, M., Lloyd, J.M., Olsen, J., Knudsen, M.F., Kuijpers, A., 2013. Early Holocene large-scale meltwater discharge from Greenland documented by foraminifera and sediment parameters. Palaeogeography Palaeoclimatology Palaeoecology 391 (A), 71–81.

Shackleton, N.J., 1974. Attainment of isotopic equilibrium between ocean water and the benthonic foraminifera genus *Uvigerina*: isotopic changes in the ocean during the last glacial. Colloques Internationaux du C.N.R.S. 219, 203–209.

Steffensen, J.P., Andersen, K.K., Bigler, M., Clausen, H.B., Dahl-Jensen, D., Fischer, H., Goto-Azuma, K., Hansson, M., Johnsen, S.J., Jouzel, J., Masson-Delmotte, V., Popp, T., Rasmussen, S.O., Rothlisberger, R., Ruth, U., Stuaffer, B., Siggaard-Andersen, M.-L., Sveinbjornsdottir, A.E., Svensson, A., White, J.W.C., 2008. Science 321 (5889), 680–684.

Stuiver, M., Grootes, P.M., Braziunas, T.F., 1995. The GISP2 ^{18}O climate record of the past 16,500 years and the role of the sun, ocean and volcanoes. Quaternary Research 44, 341–354.

Tarasov, L., Peltier, W.R., 2005. Arctic freshwater forcing of the Younger Dryas cold reversal. Nature 435, 662–665.

Thornalley, D.J.R., Elderfield, H., McCave, I.N., 2009. Holocene oscillations in temperature and salinity of the surface subpolar North Atlantic. Nature 457, 711–714.

Thornalley, D.J.R., Elderfield, H., McCave, I.N., 2010. Intermediate and deep water paleoceanography of the northern North Atlantic over the 21,000 years. Paleoceanography 25, PA1211.

Tornqvist, T.E., Hijma, M.P., 2012. Links between early Holocene ice-sheet decay, sea-level rise and abrupt climate change. Nature Geoscience 5, 601–606.

Turrell, W.R., Slesser, G., Adams, R.D., Payne, R., Gillibrand, P.A., 1999. Decadal variability in the composition of Faroe Shetland Channel bottom Water. Deep-Sea Research Part I 46, 1–25.

Vidal, L., Labeyrie, L., Cortijo, E., Arnold, M., Duplessy, J.C., Michel, E., Becque, S., van Weering, T.C.E., 1997. Evidence for changes in the North Atlantic Deepwater linked to meltwater surges during the Heinrich events. Earth and Planetary Science Letters 146, 13–27.

Walker, M.J.C., Johnsen, S., Rasmussen, S.O., Popp, T., Steffensen, J.-P., Gibbard, P., Hoek, W., Lowe, J., Andrews, J., Bjorck, S., Cwynar, L.C., Hughen, K., Kershaw, P., Kromer, B., Litt, T., Lowe, D.J., Nakagawa, T., Newnham, R., Schwander, J., 2009. Formal definition and dating of the GSSP (Global Stratotype Section and Point) for the base of the Holocene using the Greenland NGRIP ice core, and selected auxiliary records. Journal of Quaternary Science 24 (1), 3–17.

Walker, M.J.C., Berkelhammer, M., Bjorck, S., Cwynar, L.C., Fisher, D.A., Long, A.J., Lowe, J.J., Newnham, R.M., Rasmussen, S.O., Weiss, H., 2012. Formal subdivision of the Holocene

series/epoch: a discussion paper by a working group of INTIMATE (Integration of ice-core, marine and terrestrial records) and the subcommission on Quaternary stratigraphy (International Commission on Stratigraphy). Journal of Quaternary Science 27 (7), 649–659.
Worthington, L.V., 1976. On the North Atlantic Circulation. Johns Hopkins University Press, Baltimore, MD.
Wright, J.D., Miller, K.G., 1996. Control of North Atlantic Deep Water circulation by the Greenland–Scotland Ridge. Paleoceanography 11 (2), 157–170.
Wunsch, C., 2006. Abrupt climate change. An alternative view. Quaternary Research 65, 191–203.
Young, N.E., Briner, J.P., Rood, D.H., Finkel, R.C., 2012. Glacier extent during the Younger Dryas and 8.2-ka event on Baffin Island, Arctic Canada. Science 337, 1330–1333.
Yu, S.-Y., Colman, S.M., Lowell, T.V., Milne, G.A., Fisher, T.G., Breckenridge, A., Boyd, M., Teller, J.T., 2010. Freshwater outburst from Lake Superior as a trigger for the cold event 9300 years ago. Science 328 (5983), 1262–1266.